Synthetic Leaf: Economically Viable Green Hydrogen Production Using Silicon Directly from Solar Energy in an Artificial Photosynthesis Framework

Smruti Jadhav

Received January 20, 2025
Accepted March 05, 2025
Electronic access March 15, 2025

The Earth receives an astounding 173,000 terawatts of solar energy[1], surpassing global energy consumption by over 10,000 times. Unfortunately, only a fraction of this, 1 TW, immense potential is harnessed for electricity generation[2]. Additionally, the energy in the form of electricity is unsuitable for long-distance transmission, storage and mobile energy consumption requirements such as transportation. Even though electric vehicle technology is becoming a solution for ground transportation, it is unsuitable for high energy-demand transport sectors like air and maritime, which still rely on chemical energy in the form of fossil fuels. Renewable chemical energy sources, such as green hydrogen can be a potential solution for energy storage and high energy density transportation requirements. This project explores a novel & cost-effective approach inspired by nature, specifically artificial photosynthesis to produce economically viable green hydrogen. Most of the academic research in artificial photosynthesis focuses on developing an ideal semiconductor to achieve the highest efficiency in hydrogen generation with the longest possible sustained operation. Because of that, the exotic materials evaluated by such academic research are expensive and not commercially available. Silicon (Si) is not studied much since its susceptibility to immediate performance decline. This project explored using this inexpensive and commercially available semiconductors, Si, to generate hydrogen directly using solar energy. An experimental photoelectrochemical (PEC) cell was developed to measure the operational characteristics of hydrogen generation using light energy. This experiment demonstrates that inexpensive bare Si, despite exhibiting initial degradation, can settle into a steady operational regime. Economic viability calculations at this steady state suggest that if bare Si electrodes can last approximately 20 years (similar to that of existing commercial solar panels), hydrogen costs could approach $2.13/kg, a competitive price point relative to fossil-derived sources. This experimental setup not only demonstrated the feasibility of use of Si but also the economic viability of the hydrogen generation using this approach. A hydrogen generating solar panel design is proposed that can be used in large-scale hydrogen generation farms. Keywords: Artificial photosynthesis, Green hydrogen, Silicon, Photoelectrochemical cell

Introduction

Renewable energy is primarily produced in the form of electrical energy, whether from wind or solar sources. However, there are significant drawbacks to electricity compared to chemical energy, which is currently consumed in the form of fossil fuels. Electricity cannot be efficiently transported and stored, unlike fossil fuels, which can be easily transported from their origin to their consumption destination anywhere in the world. Fossil fuels can also be stored and used as needed, making them highly versatile for the transportation industry.

On the other hand, electrical energy can only be transported over short distances within a country's electrical grid system. Furthermore, storage solutions for electrical energy, such as hydroelectric pumps and battery storage, are complex and expensive, leading to transmission losses (8-15%[3]) and lower storage efficiency (80%[4]). In conventional electricity generation, these issues are often resolved by generating electricity near the location of its use and matching production to demand cycles. However, renewable energy sources such as wind and solar power lack this flexibility and are subject to the variability of natural resources.

The inability to control the amount of electricity produced and the dependency on weather conditions present significant challenges for renewable energy in the form of electricity. This has led to a growing interest in developing renewable energy sources in the form of chemical energy, which can be easily transported and stored, like fossil fuels. This shift would not only address the current limitations of renewable energy but also have positive implications for the transportation industry, as renewable fuels could be used in existing engines without requiring major infrastructure changes.

Current research is primarily centered on the potential of utilizing hydrogen as a renewable energy source. However, there is also ongoing exploration into the production of other hydrocarbons like methane to harness renewable chemical en-

ergy. This approach offers the additional advantage of reducing atmospheric CO_2 [5]. The increasing popularity of electric vehicles (EVs) has prompted a discussion about the necessity of renewable chemical energy. Despite their growing popularity, EVs currently make up only 2% [6] of the total vehicle market. This limited adoption can be attributed to several challenges. Firstly, the expensive battery technology has kept EVs in the premium segment, with no affordable options available yet. The use of costly exotic materials in battery production contributes to the high cost of EVs. Secondly, the battery power density limits the range of EVs and their suitability for long-distance travel, despite the availability of charging stations. Additionally, the charging time required for a full charge adds to travel time. Moreover, the low power density of batteries hinders their use in high-energy-demand applications such as air transportation. Even if these challenges are overcome by developing a significantly cheaper and higher energy-density battery, the lack of additional electricity grid capacity poses a third hurdle to widespread EV adoption. The US would need to invest around $500 billion [7] to modernize its grids to support broader EV adoption, and currently, there is no government plan to improve electricity grid infrastructure. Hydrogen as a form of renewable energy presents potential advantages over battery technology. It can be seamlessly integrated into existing engines with minor modifications [8], reducing initial costs. Moreover, hydrogen offers a high energy density, three times that of gasoline (A. F. 20217), which could significantly extend the range of hydrogen vehicles. For instance, the Toyota Mirai can travel up to 100 km using only 0.79 kg of hydrogen, while an average mid-size car requires 6.7 kilograms of gasoline for the same distance [9]. Additionally, hydrogen combustion results in only water vapor and zero exhaust emissions, making it an environmentally friendly option. Notably, due to this advantage, over 35,000 forklifts were already in use across US warehouses by 2019 [10]. Lastly, when utilized in fuel cells, hydrogen demonstrates high energy conversion efficiency [11], potentially opening up opportunities for its use in air transportation [12]. Hydrogen presents certain limitations, particularly in terms of its volumetric energy density. Storing a substantial quantity of hydrogen necessitates a significant volume, even under very high pressure. To provide some context, at 10,000 psi, a hydrogen storage tank would require 3-4 times the volume of gasoline tanks commonly utilized in contemporary cars [13]. Researchers are currently exploring innovative storage approaches to address this issue [14]. This research presents a novel, cost-effective approach to artificial photosynthesis that leverages widely available silicon instead of expensive semiconductor materials. While many studies emphasize efficiency, often neglecting economic feasibility, this work prioritizes stable and economically viable hydrogen production over prolonged operational periods. Specifically, I examine the performance of silicon photocathodes over multiple days, assess the stabilization of their degradation, and analyze how their sustained performance can yield significant cost advantages. Ultimately, I propose a design for scalable hydrogen-generating panels, providing a pragmatic solution for the large-scale deployment of green hydrogen.

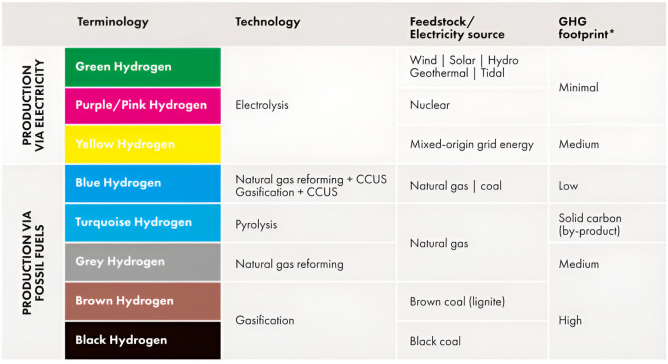

Fig.∼ 1 The Hydrogen Color Spectrum [15]

Current State of Hydrogen Production

Understanding the color system, as shown in Figure 1, for categorizing hydrogen into eight distinct color spectrums is crucial before delving into the intricacies of current hydrogen production methods.

The production methods are closely related to the amount of greenhouse gas (GHG) emissions. For example, during the production of gray hydrogen, around 12 kilograms of CO_2 are emitted into the atmosphere for every kilogram of hydrogen produced [16]. Most of the hydrogen production today is achieved by the Gasification and Steaming process with fossil fuels, which generates substantial CO_2 emissions [17]. In fact, 95% of US hydrogen produced in 2022 was from black, brown, or gray hydrogen [18], while less than one percent was green hydrogen [16].

The current green hydrogen generation process uses electricity generated from renewable sources to split water into oxygen and hydrogen using commercial electrolyzers. Figure 2 shows a typical setup of such a process. However, these systems are expensive and inefficient. Electricity generated from solar, or wind energy is not at the voltage level required by electrolyzer systems. Transformers and rectifiers convert the electricity voltage to a level that can be used by electrolyzers, leading to losses in voltage conversion components that reduces the overall efficiency. Additionally, the efficiency of the electrolysis systems is expected to be lower by $\geq$30% due to internal electric resistance [19]. As a result, the cost of green hydrogen has remained in the range of $4.5-$12 per kg, compared to $0.98-$2.93 per kg for gray hydrogen produced using natural gas [20]. Since these limiting factors associated with current green hydrogen production approach are inherently absent from a direct solar to hydrogen or artificial photosynthesis system, it is expected have

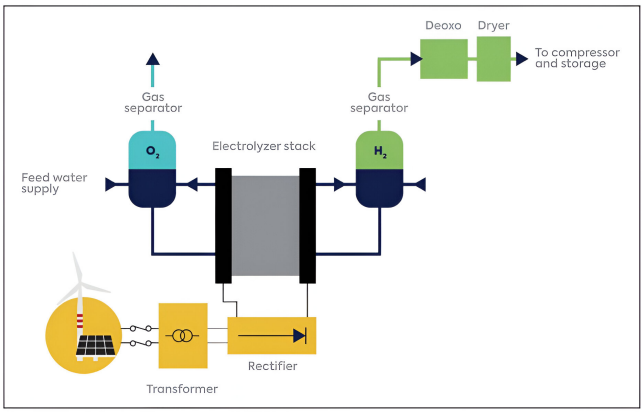

Fig.∼ 2 Green Hydrogen Production System[21]

a higher theoretical efficiency[19]. Due to these advantages, significant research is being conducted in this field of artificial photosynthesis.

Artificial Photosynthesis

Photosynthesis is a widely recognized process that is often introduced in high school curriculum. It is the method by which plants convert solar energy into chemical energy by utilizing carbon dioxide and water. Currently, the global rate of energy capture through photosynthesis is estimated at around 130 terawatts, roughly eight times the current power consumption of human civilization[22]. Within plant cells, chloroplasts harness the sun's light energy to break down water into hydrogen ions, oxygen, and electrons.

$$6H_2O + \text{photons from sunlight} \rightarrow 3O_2 + 12H^+ + 12e^- \quad (1)$$

Hydrogen ions and electrons then combine with atmospheric CO_2 to produce sugar ($C_6H_{12}O_6$).

$$6CO_2 + 12H^+ + 12e^- \rightarrow C6H12O_6 + 6O_2 \quad (2)$$

This explanation provides a simplified overview of the photosynthesis process, and details are outside the scope of this article. This simplified version facilitates the discussion of similarities and differences between natural and artificial photosynthesis. It's important to note that in natural photosynthesis, sugar and O_2 are produced rather than hydrogen, indicating that natural and artificial photosynthesis may not closely resemble each other. However, the energy required for the reactions involved in photosynthesis paints a different picture. Reaction 1 requires 1.23 eV and reaction 2 requires 0.01 eV[23]. In natural photosynthesis, 99.2% of solar energy is used to split water into hydrogen and oxygen. Therefore, replicating photosynthesis artificially depends primarily on the ability to achieve solar-driven water splitting directly. The production of carbohydrates in reaction 2 serves just nature's way of storing the hydrogen released from the water-splitting process[23].

Academic research in artificial photosynthesis involves the use of an illuminated semiconductor surface (hence, synthetic leaf), immersed in an electrolytic solution to produce hydrogen. This configuration, also known as a photoelectrochemical cell, seeks to replicate the reaction 1 using the photoelectric properties observed in semiconductors, like those used in commercial solar panels. The following section will delve into the intricate details of the photoelectrochemical cell.

Photoelectrochemical Cell (PEC)

The photoelectrochemical cell (PEC) consists of a photocathode, a p-type semiconductor wafer that acts as the cathode, and an anode made of titanium coated with ruthenium-iridium. Both the photocathode and the anode are submerged in an electrolyte solution, as depicted in Figure 3. When photons interact with semiconductors, they excite electrons from the valence band to the conduction band of the semiconductor atoms. This energy transition, known as the band gap, directly influences the water-splitting reaction and is dependent on the wavelength of the illuminating solar radiation. Each semiconductor has a unique band gap, as listed in Table 1. The visible spectrum of sunlight ranges from approximately 750 nm (red light) to 380 nm (violet light), corresponding to energy levels of 1.65 eV (red light) to 3.26 eV (violet light). It's worth noting that some semiconductors have a band gap energy that falls within the visible spectrum. For instance, Silicon (Si) has a band gap of 1.12 eV, exhibiting the photovoltaic effect for wavelengths shorter than 1107 nm, which includes the entire visible spectrum and part of the near-infrared spectrum. Conversely, some semiconductors are unsuitable for PEC due to their high band gap, only showing photovoltaic effects in the violet and ultraviolet spectra, such as Titanium Oxide.

Silicon (Si) may seem like an excellent candidate for photoelectrochemical (PEC) applications due to its ability to exhibit a photovoltaic effect in the visible light range. However, with a band gap energy of 1.12 eV, it falls short in providing the necessary energy for the water-splitting reaction. The total energy required for this reaction is at least 1.53 eV[25]. Consequently, an external bias voltage of 0.41 eV is needed to facilitate the hydrogen evolution process, as illustrated in Figure 3. While semiconductors such as InP and GaAs can produce H_2 without requiring external power, they are substantially more costly than Si, with Si priced at $16 per square foot compared to InP/GaAs at $4000 per square foot.

Once electrons are available in conduction band, they are used in the following reaction to generate hydrogen and hydroxyl ions at the photocathode.

Table 1 Semiconductor Band Gaps & Applications [24]

SemiconSemiconductorductor	Symbol	Band Gap (eV)	Application
Silicon	Si	1.12	Solar cells, electronics, microchips
Germanium	Ge	0.66	Transistors, infrared optics
Gallium Arsenide	GaAs	1.43	High-frequency electronics, solar cells
Indium Phosphide	InP	1.34	High-speed and high-frequency electronics
Cadmium Telluride	CdTe	1.44	Thin-film solar cells
Titanium Dioxide	TiO_2	3.0 - 3.2	Photocatalysis, UV detectors, solar cells
Zinc Oxide	ZnO	3.37	UV light-emitting diodes (LEDs), gas sensors
Gallium Nitride	GaN	3.4	LEDs, high-power and high-frequency devices
Silicon Carbide	SiC	2.3 - 3.3	High-temperature and high-voltage electronics
Lead Sulfide	PbS	0.37	Infrared detectors and photovoltaics
Cadmium Selenide	CdSe	1.74	Quantum dots, LEDs, photovoltaics
Aluminum Gallium Arsenide	AlGaAs	1.42 - 2.16	LEDs, laser diodes, solar cells

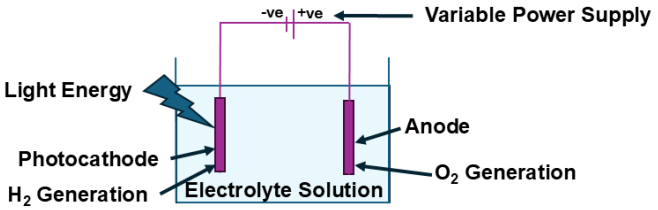

Fig.∼ 3 Photoelectrochemical Cell Setup

$$H_2O + 2e^- \rightarrow 2OH^- + 6H_2 \quad (3)$$

The hydroxyl ions are oxidized to oxygen at anode.

$$2OH^- \rightarrow H_2O + 2e^- + \frac{1}{2}O_2 \quad (4)$$

The PEC design, shown in Figure 3, is quite simple and is for illustrative purposes. However, it is unable to capture hydrogen effectively since the generated hydrogen and oxygen become mixed. To enable hydrogen capture, the cathodes and anodes are separated into different compartments. The construction process for this photoelectrochemical cell, as utilized in this study, is detailed in Materials and Methods Section.

Ongoing PEC Research

The current focus of most research is on semiconductors capable of producing hydrogen without requiring an external bias voltage. Examples of such semiconductors include InP [26, 27] , GaAs, and gallium indium phosphide (GaInP2) [25]. Photocathodes made from these materials are typically tested in electrolytes like sulfuric acid (H_2SO_4) or potassium hydroxide (KOH). It's worth noting that semiconductor material tends to corrode in strong acids or bases. For instance, InP has been observed to develop metallic oxide on its surface, necessitating platinum deposition to stabilize the oxide formation [27]. Research into surface treatments for semiconductors to prevent corrosion is also an active area of interest. In addition to platinum, nickel has also been shown to help stabilize the corrosion of Si [28]. However, these extensively studied semiconductors are quite expensive, and the additional corrosion-resistant surface treatments can impact the economic viability of hydrogen production. A more in-depth exploration of the economic viability is provided in Results Section.

When considering high-profile semiconductor candidate materials, silicon is often seen as less favorable due to two main factors: the required bias voltage for hydrogen generation and its susceptibility to corrosion. In acidic conditions, the Si photocathode was found to deteriorate to less than 10% of its original performance after 12 hours of operation [28]. Silicon is also known to react with strong bases. Hence, bases such as KOH are commonly used in the semiconductor industry for silicon etching. Some evidence suggests improved performance of Si in less corrosive electrolytes like potassium borate solution [28]. However, its long-term performance characteristics are not well researched. The degradation in performance observed up to 12 hours is unclear as to whether it continues to the complete failure of the photocathode or stabilizes over time. If its performance stabilizes, it is unknown how long it takes to stabilize or the hydrogen production rate after stabilization. This information is crucial for evaluating the economic feasibility of hydrogen production using Si. To address these questions, this study aims to conduct extended, multi-day testing of Si photocathodes.

Materials and Methods

Photocathode Fabrication

The photocathodes were produced using a modified version of the process described by [29] . The cross-section of the photocath-

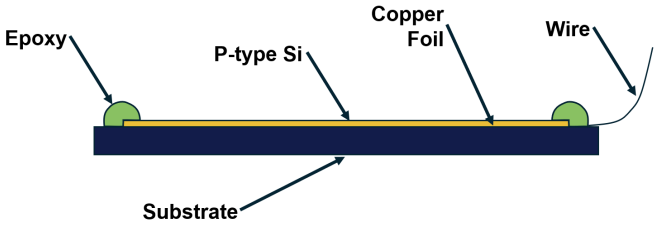

Fig.∼ **4** Photocathode Structure

ode can be viewed in Figure 4. To create the photocathode, a p-type Si wafer is attached to an insulating substrate using epoxy adhesive, with a copper foil placed in between to establish electrical contact with the back of the wafer. A wire is then soldered to the copper foil. As the assembly is exposed to a corrosive electrolyte, the creation of a secure and leak-free bond between the epoxy, substrate, and wafer is of utmost importance. Any leakage of the electrolyte and subsequent contact with electrical connections on the back side of the wafer resulted in the failure of the electrode. Overcoming the challenge of establishing a leak-free bond proved to be a significant obstacle in this research. Similar issues were also observed at National Renewable Energy Laboratory (NERL)[30].

The process of fabricating the photocathode is illustrated in Figure 5. Two substrates (glass, 1/8" x 2.5" x 4" and acrylic sheets, 1/4" x 2.5" x 4") and five types of epoxy adhesives (Henkel 9460, 1C-LV, 1C, E-40HT, AA 3035) were tested to assess the electrolyte leakage. The best leak-free operation was provided by acrylic sheets with Henkel 1C, which were selected as the final design. To increase the adhesion to the epoxy, the acrylic sheet was first roughened and then cleaned with water and dried. The dried surface was cleaned with methyl alcohol. The adhesive copper foil (Amazon, ELK Copper Foil Tape, 2" wide) was attached to the cleaned surface, as shown in Step 1 of Figure 5, and an electrical wire was soldered to one end of the foil, as shown in Step 2. The Si wafer (p-type, 3" diameter, 0.4 mm thickness, 100 orientation, conduction side - Ti 5nm/Ag 350nm) was cleaved to the required size using a diamond scribe (Ted Pella Item # 54483). Hydrofluoric acid (HF) is typically used to clean Si wafers to remove silicon dioxide (SiO_2) residues. However, due to the absence of access to a facility equipped to handle highly toxic hydrofluoric acid (HF), glass etching paste (Amazon, Armor Etch) was used to clean Si wafers. This paste was also effective in removing SiO_2 from wafer. A silver conductive paint (Ted Pella Item # 16062-15) was applied to the copper foil, covering all areas except the edges. This conductive paint allowed conductive contact between the conductive side of the wafter and the copper tape. The conduction side of the wafer was placed on the painted foil, as shown in Step 3. Before applying the epoxy adhesive in Step 4, the wafer, substrate, and electrical connections were cleaned with methyl alcohol. Extra precaution was taken to ensure that no edges or electrical

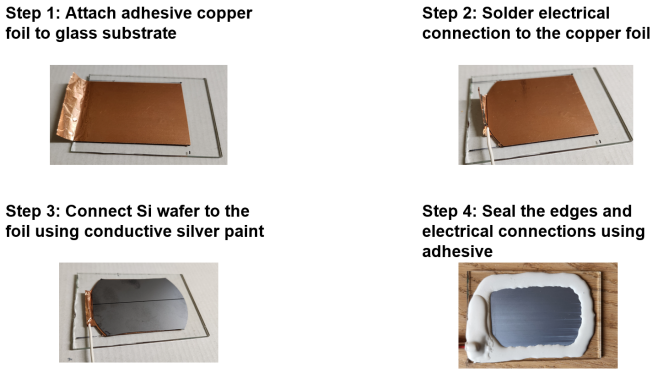

Fig.∼ **5** Photocathode Fabrication

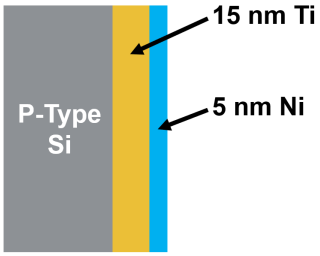

Fig.∼ **6** Ni/Ti Coating on P-Type Silicon

contacts remained uncovered by the epoxy.

Two types of photocathodes were fabricated using bare silicon and Nickel-titanium (Ni/Ti) coated Si to compare the performance and cost-effectiveness of both approaches for hydrogen generation. Research has demonstrated that the performance of Ni/Ti coated Si is superior to that of bare silicon[28]. A 15 nm Ti adhesion layer and a 5 nm Ni layer were deposited utilizing an Angstrom Engineering Physical Vapor Deposition system (Model EVOVAC 008) at Rutgers Nanofabrication Core Facility as shown in Figure 6

Experimental Setup

A commercially available H-Type electrolytic cell (StonyLab, Part Number: SL000199, 500ml) was converted into a photoelectrochemical cell (PEC), as illustrated in Figure 7. This electrolytic cell was selected since it could fit the photocathode and anode. The photocathode and anode, composed of titanium coated with ruthenium-iridium (Amazon, Tibromtack, 0.04" x 2" x 4"), were placed in separate compartments within the PEC to avoid the mixing of O_2 and H_2. This setup allowed for the measurement of H_2 generation. A photography light (Amazon, Neewer, MS150B, 200000 lux/0.5m, CRI97+) equipped with a spotlight modifier (Amazon, Wellmaking) was utilized to concentrate the light on the small area of the photocathode, approximately 2 x 3 inches in size. A light intensity of 140k lux

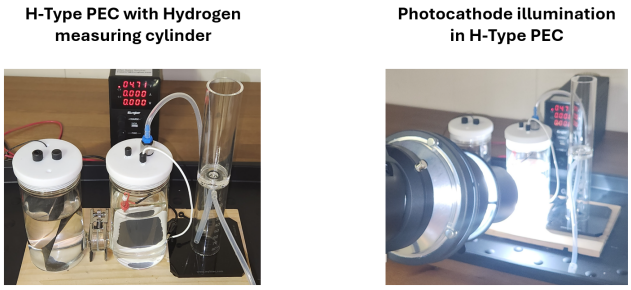

Fig.∼ 7 PEC Experimental Setup

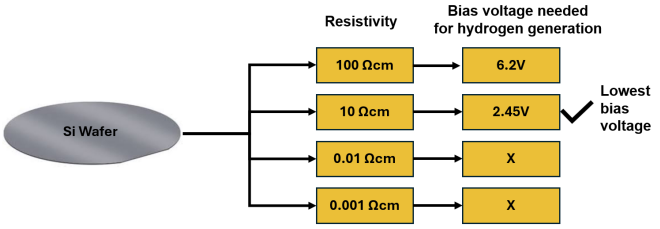

Fig.∼ 8 Si Resistivity and No-Light Zero Current Bias Voltage

Fig.∼ 9 Failure of Photocathode in KOH Electrolyte

was achieved near the PEC, as confirmed using a light meter (Amazon, Urceri, 200,000 Lux). This test demonstrated that the experimental setup could replicate the intensity of sunlight, which typically measures around 100k lux. A hydrogen measuring cylinder (H-Tech Education, Storage 80, 80 ml) was connected to the cell compartment containing the photocathode to measure the volume of hydrogen generated. A variable power supply (Amazon, Kungber, 30V 10A) was connected between the photocathode and the anode to enable adjustment of the bias voltage across the photocathode and anode, which is necessary to provide the additional energy required for water splitting. It should be noted that the photovoltaic effect by Si cannot generate all the energy needed for water splitting. Various plumbing and electrical adaptors and connectors sourced from Amazon and McMaster-Carr were used to interconnect all the components.

Optimal Silicon resistivity Selection

P-type silicon, which is used to fabricate the photocathode, is produced by introducing impurities (doping) of elements from Group III of the periodic table. The most commonly used doping elements are Boron, Gallium, and Indium. The doping concentration in the silicon wafers affects their resistivity and the performance of the photoelectrochemical cell (PEC). As the doping concentration increases, the resistivity of the wafers decreases, as does the required bias voltage, up to a certain point. Beyond this level, if the doping concentration continues to increase, the silicon begins to behave like a metal and loses its ability to produce the photovoltaic effect. This overly doped silicon is referred to as degenerately doped.

Four different silicon wafers with resistivity values of 100, 10, 0.01, and 0.001 cm were tested, and the bias voltage was recorded (see Figure 8). When the PEC light source was turned off, the voltage on the variable power supply was gradually increased until the current remained just below zero amps. The 0.01 and 0.001 cm wafers did not exhibit any photovoltaic effect and were unable to produce hydrogen. Among the 100 and 10 cm wafers, the latter had the least bias voltage requirement and was therefore selected for the final experiment.

Electrolyte Selection

In the initial tests, a 1M potassium hydroxide (KOH) electrolyte was used. The solution was prepared by dissolving 56.11 g of KOH in 1 liter of distilled water. Because Si reacts with KOH, it was anticipated that the performance of the photocathode would degrade. Nevertheless, this test was conducted as part of the research objective to determine whether the degradation stabilizes over time or leads to photocathode failure, along with the corresponding timeline. The photocathode indeed failed within one day of operation. The KOH electrolyte slowly eroded the Si, impacting its structural integrity and causing the wafer to detach from the epoxy joint, as illustrated in Figure 9.

Potassium borate buffer[28]has been shown to be less corrosive, hence used in the next set of tests. The electrolyte was prepared using 1M KOH and 2M boric acid solution. 64 g of boric acid was dissolved in 1 liter water to make 2M boric acid solution. Photocathode survived 7-day continuous operation in this electrolyte after which the experiment was stopped

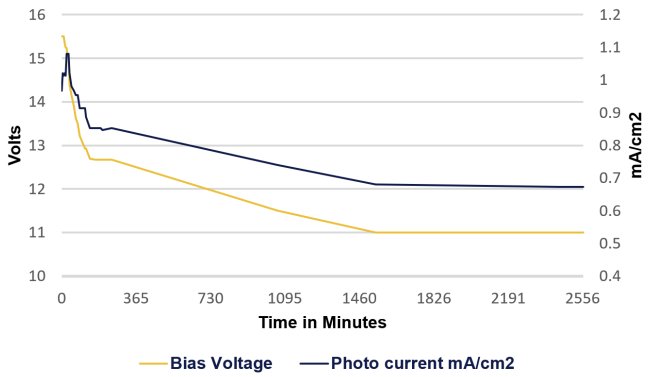

Fig.∼ 10 Performance of Si - Potassium Borate Buffer

Test Procedure

The experiment was conducted at room temperature, focusing on two key parameters: the no-light zero current bias voltage, which served as the control parameter, and the photocurrent generated upon illumination of the photocathode, alongside hydrogen generation, which were the measured parameters. The experimental setup utilized commercially available products rather than specialized lab-grade equipment, which may represent a limitation and a potential source of error in the results. For instance, high-quality sun simulation lights that accurately replicate the spectrum of natural sunlight typically cost $5,000 or more. In this experiment, a photography light with a Color Rendering Index (CRI) of 97 was employed. Achieving a visible light spectrum that closely resembles that of sunlight is crucial for excellent color rendering. Hence, it can be assumed that this light can approximate the visible spectrum of sunlight. As a result, it is expected that the measured and calculated parameters may exhibit slight discrepancies when compared to those obtained with lab-grade light. At the same time, the overall conclusion of the experiment is expected to remain the same. The initial step involved adjusting the no-light zero current bias voltage to maintain the current just below zero amps with the light off. Upon turning on the light, bubbles began to appear on the surface of the photocathode, and photocurrent readings were observed on the ammeter of the power supply. The values for the no-light zero current bias voltage (in volts) and photocurrent (in milliamps) were noted as shown on the variable power supply. Initially, this process of bias voltage adjustment and parameter measurement was repeated every 30 minutes. These values were recorded for the first three days and remained constant from Day 3 onwards. The photocurrent is converted to current per cm^2 area of photocathode. The data collected is presented in Figure 10. Confirmation of hydrogen generation was obtained by collecting hydrogen in soap water bubbles and conducting controlled ignition tests.

A rapid decrease in the no-light zero current bias voltage and photocurrent was initially observed, but it stabilized after 24 hours. This decrease may be attributed to electrolytes modifying the Si surface[30]. Subsequently, this decline stabilized after 24 hours, and the parameters remained at the stabilized level for seven days. Hydrogen was generated at a rate of 25 ml per hour when the zero current bias voltage and photocurrent stabilized.

Similar tests were conducted using a photocathode made of Ni/Ti coated Si for comparative analysis. No decline in performance was observed with Ni/Ti coated Si, which is consistent with findings from[28]. The rate of hydrogen generation increased to 40 ml per hour, representing a 60% improvement. It is essential to note that while this improvement is significant, the hydrogen generation rate alone does not fully indicate the economic viability of both approaches. Consequently, the subsequent section will conduct a thorough cost analysis of both approaches and assess the resulting cost of hydrogen production, a critical consideration for practical application.

Results

Table 2 shows a performance analysis of the photocathodes produced using Si and Ni/Ti-coated Si. The first two points have been previously covered and are included here for completeness. This section delves into the economic viability of both approaches by assessing the cost of hydrogen production and the payback period. The cost estimation is based solely on the wafer cost and does not encompass additional expenses such as extra energy requirements (bias voltage), manufacturing, and maintenance costs. These additional costs are assumed to be equal for both methods and thus do not affect the relative comparison.

The cost of $16 per square foot for bare Si was determined using bulk solar grade wafer pricing from online vendors[31]. This cost is assumed to be constant over time, but the real-world wafer prices can fluctuate based on market demand. The Rutgers Nanofabrication Core Facility, where the Ni/Ti coating was applied, was unable to provide an estimate for the commercial cost of such coating. Estimates were obtained from commercial providers, with the lowest estimate being $160 per square foot. Large scale coating cost can be significantly reduced, but the conclusion of this study would not change even with a 50% coating cost reduction. These cost estimates for the wafers were then used to calculate the cost of hydrogen production, as shown in Table 3. The calculations assume a one-year lifespan for both photocathodes. Total area of photocathode is assumed to be 1 m^2. The volumetric mass density of gaseous hydrogen at atmospheric pressure and 20°C of 0.083 kg/m³ was used to calculate mass. It is apparent that even with a 60% improvement in hydrogen generation with the Ni/Ti-coated Si photocathode, the cost of H_2 rises to $266.48 per kg compared to $42.64 for bare Si. This increase is primarily due to the cost of the Ni/Ti coating. Another avenue for further research in artificial photosynthesis

Table 2 Si vs Ni/Ti Coated Si Photocathode Performance Comparison

Silicon	**Nickel/Titanium Coated Silicon**
Performance decline for 24 hours and stabilized after that	No performance decline for 24 hours
H_2 production - 25 ml per hour	H_2 production - 40 ml per hour
Cost of wafer - $16 per sq ft	Cost of wafer - $160 per sq ft
1 year life H_2 cost - $42 per kg	1 year life H_2 cost - $266 per kg
Life for commercial cost (∼$5) – 8 Years	Life for commercial cost (∼$5) – 50 Years

involves the utilization of high-performance semiconductors, such as InP or GaAs, which operate without the need for bias voltage. These materials show promise, but their limited accessibility and high cost, reaching up to $4000 per sq foot, may restrict their practical use in commercial applications. Over time, this cost is expected to decrease as technology evolves, but it must be significantly lower to be comparable to Si.

There is currently no experimental data available regarding the overall life expectancy of both approaches. Assuming a 1-year life expectancy is considered overly simplistic. An analysis of the payback period was conducted to determine how long a photocathode needs to survive to be economically viable. The payback period is the time required for the hydrogen production revenue to offset the initial PEC system cost. It directly determines whether a PEC system can achieve an economically viable hydrogen cost of around $5 per kg, approximately equal to the current green hydrogen cost, within an investment timeframe acceptable to the industry. This $5 economic viability threshold is assumed to be constant over time. The detailed calculations can be found in Table 4.

The Si photocathode is expected to have a lifespan of just eight years in order to produce hydrogen at $5.33 per kg, compared to the 50-year lifespan of Ni/Ti-coated Si. For context, commercial photovoltaic solar panels typically last between 20 and 30 years. It is unrealistic to expect that Ni/Ti-coated Si photocathodes will last 50 years. Conversely, if the bare Si photocathode can last for 20 years, similar to the lifespan of current solar panels, the cost of hydrogen production could decrease to $2.13 per kg. These calculations may be considered oversimplified and theoretical. Nevertheless, they indicate the potential for bare Si in hydrogen production when compared to other costly methods. If the stable performance observed during the 7-day test can be maintained over multiple years, hydrogen could be produced at an economically feasible cost due to the extremely low price of Si.

Future Work

The PEC design utilized in this research is not suitable for large-scale hydrogen production. Furthermore, it has been observed that the proximity of the photocathode and anode is pivotal for efficient hydrogen generation. Based on these findings, a panel-like design (refer to Figure 11) is proposed. Strips of p-type Si and anode will be positioned close to each other but separated by an anion exchange membrane to prevent the mixing of hydrogen and oxygen. Potassium borate or a similar less corrosive electrolyte can be used in the narrow space between the photocathode and anode. The sun-facing side of the anode will be equipped with a photovoltaic cell that will harness sunlight to generate the bias voltage required for hydrogen production. Hydrogen will be collected from the photocathode section of the panel. Such a panel design has the ability to capture solar irradiance on its entire surface. While the anode's sun-facing surface does not contribute to photovoltaic activity, it is augmented by a photovoltaic layer. This addition allows for the utilization of otherwise unexploited solar irradiance. Notably, the electricity generated by this PV layer can provide the necessary bias voltage for water splitting, thereby eliminating the reliance on an external power source. This self-contained design has the potential to considerably reduce the initial investment requirements for large-scale hydrogen production facilities, as it circumvents the need for extensive external power infrastructure

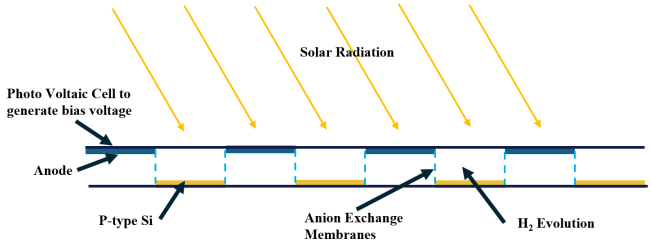

Fig.∼ 11 Proposed Commercial PEC Panel Design

Such panels need to undergo long-term multi-year performance testing. Multiple such long-lasting PEC panels can be installed in high annual solar radiation areas to form hydrogen farms, similar to the configuration of current solar farms. The hydrogen generated from each PEC panel can be gathered at a central location and then transported to various destinations for use as fuel in internal combustion engines, hydrogen fuel cells, and other applications.

Table 3 Hydrogen Cost Calculation for 1 Year Life Assumption

Si Type	Hydrogen Production ml/hour	Wafer area cm^2	Kg of H_2 per hours per m^2	Lifetime in year	Kg of H_2 produces during the life	Cost of wafer per Sq Ft	Cost of H_2 during the lifetime \$/kg
Si	25	15	0.0014	1	4.04	16	42.64
Ni/Ti Si	40	15	0.0022	1	6.46	160	266.48

Table 4 Payback Period Analysis

Si Type	Hydrogen Production ml/hour	Wafer area cm^2	Kg of H_2 per hours per m^2	Lifetime in year	Kg of H_2 produces during the life	Cost of wafer per Sq Ft	Cost of H_2 during the lifetime \$/kg
Si	25	15	0.0014	8	32.31	16	5.33
Ni/Ti Si	40	15	0.0022	50	323.15	160	5.33

Conclusion

The research compares the efficiency and cost-effectiveness of two methods for hydrogen generation: using uncoated silicon (bare Si) and silicon coated with Ni/Ti. The latter method represents various similar approaches that employ advanced coating techniques or semiconductor materials known to outperform bare Si but at a higher cost. The research showed that while the performance of bare Si initially decreased, as noted in previous studies, it stabilized after 24 hours and remained consistent over the seven-day testing period. Despite the degradation, the hydrogen production at this stable level could potentially be economically viable due to the widespread availability and low cost of Si. Strategies to enhance Si performance, such as Ni/Ti coating, or the use of alternative high-performance semiconductors like InP or GaAs, are extremely expensive and render commercial applications unfeasible. If the stabilized performance of Si observed in this research can be maintained for at least eight years, it could lead to economically viable hydrogen production at \$5 per kg, similar to current green hydrogen cost. Further research is necessary to assess the long-term performance of this approach using the proposed hydrogen-generating panel design. These panels could offer a practical artificial photosynthesis-based solution for introducing green hydrogen to the market until more efficient methods become viable.

Acknowledgement

The author expresses gratitude to Dr. Todd Deutsch from the National Renewable Energy Laboratory, Dr. Weilai Yu from Stanford University, and John M. Evans from the California Institute of Technology for their invaluable guidance throughout the research. The author also extends thanks to Dr. Ngwe Zin from the Rutgers Nanofabrication CORE Facility for facilitating the Ni/Ti vapor deposition on Si and allowing the process to be shadowed.

References

1 NASA, *Earth Fact Sheet*, 2024, https://nssdc.gsfc.nasa.gov/planetary/factsheet/earthfact.html.

2 IRENA, *Renewable Capacity Statistics 2023*, 2023, https://www.irena.org/Publications/2023/Mar/Renewable-capacity-statistics-2023.

3 *How Much Power Loss in Transmission Lines*, Chint Blog, 2021, https://chintglobal.com/blog/how-much-power-loss-in-transmission-lines/, Accessed: 2025-03-21.

4 U. E. I. Administration, *Utility-scale Batteries and Pumped Storage Return about 80% of the Electricity They Store*, 2021, https://www.eia.gov/todayinenergy/detail.php?id=46756.

5 S. Yu and P. K. Jain, *Nature Communications*, 2019, **10**, year.

6 I. E. Agency, *Global EV Data Explorer – Data Tools*, 2024, https://www.iea.org/data-and-statistics/data-tools/global-ev-data-explorer.

7 A. A. Forum, *The Cost of Upgrading Electric Distribution*, 2021, https://www.americanactionforum.org/research/the-cost-of-upgrading-electric-distribution/.

8 W. Lanz, *Hydrogen Use in Internal Combustion Engines*, 2001.

9 T. Europe, *LCA — 2nd Generation Toyota Mirai*, 2021, https://www.toyota-europe.com/sustainability/carbon-neutrality/vehicle-life-cycle-assessments/lca-2nd-generation-mirai.

10 U. D. of Energy, *10 Things You Might Not Know About Hydrogen and Fuel Cells*, 2019, https://www.energy.gov/eere/articles/10-things-you-might-not-know-about-hydrogen-and-fuel-cells.

11 A. F. D. Center, *Hydrogen Basics*, 2021, https://afdc.energy.gov/fuels/hydrogen-basics.

12 Airbus, *The Green Hydrogen Ecosystem for Aviation, Explained*, 2021, https://www.airbus.com/en/newsroom/news/2021-06-the-green-hydrogen-ecosystem-for-aviation-explained.

13 Fuel Cell Technologies Office, *Hydrogen storage*, https://www.energy.gov/eere/fuelcells/hydrogen-storage, 2017, U.S. Department of Energy.

14 *Materials-Based Hydrogen Storage*, Energy.gov, 2015, https://www.energy.gov/eere/fuelcells/materials-based-hydrogen-storage, Accessed: 2025-03-21.

15 *Hydrogen – Data Telling a Story*, Global Energy Infrastructure, 2021, https://globalenergyinfrastructure.com/articles/2021/03-march/hydrogen-data-telling-a-story/, Accessed: 2025-03-21.

16 MIT Climate Portal, *How Clean is Green Hydrogen?*, 2024, https://climate.mit.edu/ask-mit/how-clean-green-hydrogen, Accessed: 2024-03-12.

17 M. Zhang and X. Yang, *Sustainability*, 2022, **14**, 9700.

18 R. Mills, *Clean Energy 101: The Colors of Hydrogen*, RMI, 2022, https://rmi.org/clean-energy-101-hydrogen/.

19 A. Rothschild and H. Dotan, *ACS Energy Letters*, 2017, **2**, 45–51.

20 K. Schelling, *BloombergNEF*, 2023.

21 A.-S. Corbeau and A.-K. Merz, *Center on Global Energy Policy at Columbia University SIPA — CGEP*, 2023.

22 Wikipedia contributors, *Photosynthesis*, 2024, https://en.wikipedia.org/w/index.php?title=Photosynthesis&oldid=1225382799, [Online; accessed 2024-03-12].

23 D. G. Nocera, *Accounts of Chemical Research*, 2012, **45**, 767–776.

24 S. M. Sze, Y. Li and K. K. Ng, *Physics of Semiconductor Devices*, 2021.

25 J. Head and J. Turner, *Journal of Undergraduate Research*, 2007, **7**, year.

26 E. Aharon-Shalom and A. Heller, *Journal of The Electrochemical Society*, 1982, **129**, 2865–2866.

27 W. Yu, M. H. Richter, P. Buabthong, I. A. Moreno-Hernandez, C. G. Read, E. Simonoff, B. S. Brunschwig and N. S. Lewis, *Energy & Environmental Science*, 2021, **14**, 6007–6020.

28 J. Feng, M. Gong, M. J. Kenney, J. Z. Wu, B. Zhang, Y. Li and H. Dai, *Nano Research*, 2015, **8**, 1577–1583.

29 O. J. Alley, K. Wyatt, M. A. Steiner, G. Liu, T. Kistler, G. Zeng, D. M. Larson, J. K. Cooper, J. L. Young and T. G. Deutsch, *Frontiers in Energy Research*, 2022, **10**, 884364.

30 T. Deutsch, *Semiconductors for photoelectrochemical water splitting*, 2024, [Personal Communication].

31 Buy Solar Online, *Buy Solar Online*, 2024, https://order.universitywafer.com/default.aspx?cat=Solar.